Variability of chromophoric dissolved organic matter in three freshwater-influenced systems along central-southern Chile

Angel Rain-Franco, Marcus Sobarzo, Jocelyne Caparros, Camila I. Fernandez

Variability of chromophoric dissolved organic matter in three freshwater-influenced systems along central-southern Chile.

Angel Rain-Franco [a*], Marcus Sobarzo [b, c], Jocelyne Caparros [c] & Camila Fernandez [c, d, e, f]

[a] Graduate Program in Oceanography, Department of Oceanography, Faculty of Natural Sciences and Oceanography, Universidad de Concepción, P.O.Box 160-C, Concepción, Chile

[b] Department of Oceanography, Universidad de Concepcion, Casilla 160-C, Concepcion, Chile

[c] Sorbonne Université, UPMC Univ Paris 06, Laboratoire d'Océanographie Microbienne (LOMIC), Observatoire Océanologique de Banyuls/Mer, F-66650, Banyuls/Mer, France

[d] Center for Interdisciplinary Aquaculture Research (INCAR), Universidad de Concepción, Chile

[e] Centro de Investigación Oceanográfica COPAS Sur-Austral, Universidad de Concepción, Chile

[f] Centro Fondap de Investigación Dinámica de Ecosistemas Marinos de Altas Latitudes (IDEAL), Valdivia, Chile

*Present address: Sorbonne Université, UPMC Univ Paris 06, Laboratoire d'Océanographie Microbienne (LOMIC), Observatoire Océanologique de Banyuls sur Mer, F-66650, Banyuls/mer, France

E-mail addresses: rain.angel@obs-banyuls.fr (A. Rain-Franco), msobarz@udec.cl (M. Sobarzo), jocelyne.caparros@obs-banyuls.fr (J. Caparros), fernandez@obs-banyuls.fr (C. Fernandez, corresponding author).

Abstract

Chromophoric dissolved organic matter (CDOM) is a biologically active component of dissolved organic matter that influences the optical properties of aquatic environments, thereby playing an important role in the photochemical and photobiology processes occurring in the euphotic layer. Three cruises were carried out at three contrasting oceanographic areas off central and southern Chile (36.8°S, 44.6°S, 54.9°S) between November 2013 and July 2017 in order to assess the variability of the CDOM pool's optical properties (a_{325}, S_{CDOM}, S_R). Marked differences, including vertical variability, were found for a_{325}, S_{CDOM}, and S_R within and among each of the three zones, although surface DOC concentrations remained constant at all sites (87.59 ± 26.04 µmol L^{-1}). At the coastal area close to the Biobio River (36.8ºS), a_{325} values varied between 0.26-1.93 m^{-1} with maximum measured in surface waters. For the Puyuhuapi fjord in northern Patagonia (44.6ºS), a_{325} ranged between 0.69 and 3.86 m^{-1}, while in the Beagle Channel (54.9ºS) it oscillated between 0.59 and 1.73 m^{-1}. We identified the terrestrial organic matter input to surface waters as the main factor influencing surface CDOM concentrations in central Chile. In the Puyuhuapi fjord, terrestrial influence was heterogeneous because of its seasonal variability of the Channel but it was overall less significant than *in situ* produced CDOM. We also observed the lowest contribution of terrestrial CDOM inputs compared to the *in situ* production in southern Patagonia (Beagle Channel). We observed that the distribution of CDOM is potentially dominated by biological *in situ* production below the surface freshwater-influenced layer in the southern area while highly influenced by terrestrial input in the coastal upwelling area at 36ºS.

Overall, this study shows that the optical properties of dissolved organic matter (mainly SR) can be suitable for identifying different CDOM pools in coastal areas of contrasting oceanographic conditions. In stratified systems, freshwater inputs determine the distribution of surface CDOM while in well-mixed conditions, the *in situ* production determine the general CDOM concentration.

Keywords: CDOM, DOC, central Chile, northern Patagonia, southern Patagonia

1. Introduction

Chromophoric dissolved organic matter (CDOM), the fraction of dissolved organic matter (DOM) that interacts with solar radiation and absorbs ultraviolet and visible radiation (Bricaud et al., 1981), is an ubiquitous compound in the marine water column (Nelson and Siegel, 2013). It is produced by the microbial degradation of biologically produced dissolved organic carbon (DOC) (Nelson et al., 1998). Experimental evidence shows that zooplankton (Steinberg et al., 2004) and macroalgae (Hulatt et al., 2009) can release significant amounts of CDOM. In coastal environments, CDOM has primarily terrestrial origins and shows a rapid decline across the continental shelves (Vodacek et al., 1997) primarily via the photochemical alteration or photobleaching of CDOM. This process is dependent on incident solar radiation and water column stratification (Vodacek et al., 1997; Del Vecchio and Blough, 2004).

Several optical approaches, including absorbance and fluorescence, have been used to describe the dynamics relationship between DOC and CDOM because its optical properties, especially those based on the absorption spectra, help identifying the origins of CDOM in aquatic ecosystems (Helms et al., 2008; Hansen et al., 2016). Some studies have used absorption spectra to predict potential changes in coastal DOC concentrations (Fichot and Benner, 2011), revealing the importance of CDOM river discharges into the coastal ocean and the seasonal significance of photochemical degradation (Mannino et al., 2008).

The coastal area off central Chile is characterized by seasonally variable rates of biological production and chlorophyll concentration, with maximum levels related to wind-driven

upwelling in spring-summer (Yuras et al., 2005) and minimum levels dominated by freshwater inputs (mainly riverine) in winter (Escribano and Schneider, 2007). The strong discharge of the Biobío River (Saldías et al., 2012) represents over 40% of the region's marine DOC in winter and spring in this area (Vargas et al., 2013; Fig. 1A) which produces strong physical and chemical gradients in the water column on short spatial scales (Vargas et al., 2013).

Northern and southern Patagonia (41-55ºS) comprise geographically complex channels, fjords, and bays where freshwater continental waters (coming from rivers, precipitation and snow/glacier melting) interact with marine waters (Iriarte et al., 2014). Primary production shows a southward latitudinal gradient, going from 0.089-0.372 gC $m^{-2}d^{-1}$ (North) to 0.114-0.120gC $m^{-2}d^{-1}$ (South). Because of the high correlation between photosynthetically active radiation (PAR) and primary productivity throughout Patagonia, some authors have recognized the importance of CDOM in the attenuation of PAR (Jacob et al., 2014) and even UV radiation in the area (Houvinen et al., 2016).

Using these three contrasting study areas, this study aims to evaluate the contribution of terrestrial-derived CDOM as a function of freshwater inputs and stratification levels and to analyze the variability of CDOM using its optical parameters.

2. Materials and methods

2.1. Study area and sampling strategy

105 Three oceanographic cruises were carried out at contrasting study areas: 1) at the mouth of
106 the Biobio River, in the coastal upwelling area off central Chile (36.8°S; November 2013),
107 2) the Puyuhuapi Fjord in northern Patagonia (44.6°S; August 2016) and 3) the Beagle
108 Channel in southern Patagonia (subantarctic region; 54.9°S; July 2017; Fig. 1).
109 The Biobio station was visited for 27 hours, with samplings scheduled every 3 and then
110 every 6 hours (six profiles total; Fig. 1A). Four stations were sampled along a transect from
111 Jacaf Channel to the southern mouth of Puyuhuapi Channel in Puyhuapi ford (Fig. 1B).
112 This area is characterized by a seasonal stratification. Inside the fjord, the winter input of
113 marine water comes strongly from the north via the Jacaf Channel while freshwater comes
114 from the Cisnes River, in the central part of the Puyuhuapi Channel. This creates a well-
115 mixed water column (Fig. 1B). However, in spring-summer, the water column is highly
116 stratified, driven by freshwater discharges in the northern part of Puyuhuapi fjord
117 (Schneider et al., 2014). In the Beagle Channel we concentrated in two subantarctic fjords:
118 Yendegaia and Pia (Fig. 1C). Yendegaia shows a retreated glacier separated from the fjord
119 by ~12 km, whereas Pia Fjord receives freshwater inputs directly from a glacier. In each
120 fjord three stations were sampled on a transect going from the head to the mouth of each
121 fjord (Table 1).
122
123 The physico-chemical variability of the study areas was assessed with CTD profiles
124 (SeaBird®). Seawater samples were collected using Niskin bottles. Surface sampling (1 m)
125 was carried out by closing the Niskin bottle immediately below the surface (Table 1).
126 The mean daily river discharge data were obtained from the Dirección General de Aguas
127 (www.dga.cl). Data was used between January 2007 and December 2012 for the Biobio
128 River (Central Chile) and between January 2007 and December 2014 the Cisnes River in

129 the Puyuhuapi Fjord (Northern Patagonia). There is not data available for the Beagle
130 Channel.

131 We estimated the degree of stratification of the water column for each profile using the
132 stratification parameter, ns, defined by Haralambidou et al., (2010) and applied previously
133 by Schneider et al ., (2014) for Puyuhuapi as shown in equation 1:
134
135 $$ns = S_{50m}\text{-}S_{surface} / ½ (S_{50m}+S_{surface}) \qquad (1)$$
136
137 Where $S_{surface}$ and S_{50m} are defined as the salinity at surface m and 50 m, respectively.
138 Surface salinity for Biobío corresponds to values at 1m, for Puyuhuapi at 2m and for
139 Beagle at 0.5 m depth. The stratification parameter varies from values lower than 0.1
140 (representing a well-mixed water column), between 0.1-1 (partially mixed) and higher than
141 1 (highly stratified water column).
142
143 Bacterioplankton abundances (including archaea and bacteria) were estimated by flow
144 cytometry (Marie et al., 2000) using a FACSCalibur flow cytometer at Universidad de
145 Concepcion. Samples were taken in duplicate using sterile cryovials (1350 µL), fixed with
146 glutaraldehyde (0.1% final concentration), and stored at -80°C until laboratory analysis.
147
148 For DOC samples, water was filtered using GF/F filters (0.7 µm, combusted at 450°C, 6 h)
149 and sterile syringes. Samples were stored in glass vials (previously combusted at 450°C, 6
150 h) and acidified immediately with H_3PO_4 (25%; 90µL/15mL) to pH 2. DOC concentrations
151 were determined by chromatography using a Shimadzu TOC-5000 carbon analyzer (Benner
152 and Strom, 1993) at the laboratory of microbial oceanography (CNRS, France).
153

Samples for nitrate (NO_3^-) and nitrite (NO_2^-) determination were taken in duplicate (10 mL) and stored at -20°C awaiting colorimetric analysis with a Brann Luebbe® autoanalyzer (Aminot and Kérouel, 2007). Total chlorophyll-a (Chl-a) was estimated using a Turner Design fluorometer (Holm-Hansen et al., 1965). CDOM was sampled in duplicate (50 mL) and slowly filtered through precombusted GF/F filters (0.7 µm 450°C, 6 h). Samples were then stored in dark conditions at -20°C until absorption analysis.

Absorbance for CDOM determination was measured in an Agilent 8453 UV-Visible spectrophotometer (single beam spectrophotometer). CDOM concentrations were determined using the absorption spectra at 325 nm as a proxy (Nelson et al., 2007; Swan et al., 2009). Ultrapure water was used as a blank. The absorption coefficient was according to equation 1 (Bricaud et al., 1981):

$$\alpha_{CDOM(\lambda)} = 2.303\, A_{(\lambda)} / L \qquad (2)$$

where α_{CDOM} is the absorption coefficient (m^{-1}), A is the absorption of the sample (325 nm), and *L* is the optic length path (0.05 m). A baseline correction was applied by subtracting the absorption at 700 nm.

The spectral slope (S_{CDOM} in nm^{-1}) was estimated at intervals of 300 to 700 nm of absorption spectra through a simple exponential function fitted using a non-linear regression (Twardowski et al., 2004) according to equation 3:

$$\alpha_{(\lambda)} = \alpha_{(\lambda Ref)} * \exp\,(-S*(\lambda - \lambda ref)) \qquad (3)$$

where α is the absorption coefficient (m^{-1}), λ is the wavelength (nm), and λ_{ref} is the reference wavelength (300 nm). Additionally, we calculated the slope ratio (S_R) between spectral slopes at 275-295 nm ($S_{275-295}$) and 350-400 ($S_{350-400}$) using a linear regression to the natural log-transformed spectra (Helms et al., 2008).

178

179 **2.2. Statistical analyses**

180

181 Principal component analysis (PCA) was performed using environmental variables
182 (temperature, salinity, nitrate, bacterioplankton and *Synechoccocus sp* abundances, Chl-a)
183 in order to reduce dimensionality and then compare with a_{325} values by area. We did several
184 linear regressions between the first and second principal component scores and a_{325}. The
185 significance of each regression was tested using the lm function. Several Spearman
186 correlation tests were calculated to assess potential relationships among a_{325} and DOC in
187 each study zone. Finally, a Wilcoxon pairwise comparison was used (R-package lattice) to
188 test significant differences of DOC concentrations, a_{325}, S_{CDOM}, and S_R by zone and layers.
189 The statistical analyses were performed with the software R (https://www.r-project.org/).

190

191 **3. Results**

192

193 **3.1. Oceanographic conditions**

194

195 In central Chile, monthly averages of freshwater discharge of the Biobío River show
196 variable outflow though the year, reaching maxima in the spring months (1494 ±853 m^3 s^{-1}
197 during August), while minima were observed during early autumn (320 ± 172 m^3 s^{-1} in
198 April). Monthly average for November was 989 ± 430 m^3 s^{-1} (Fig.2A). Consequently, the
199 water column was stratified in the first 5 m, presenting surface (1 m) temperatures of 16.75
200 ± 1.05 °C and salinity of 21.36 ± 2.55 psu. Below this surface layer, salinity remained
201 constant (~35 psu), whereas temperature decreased slowly with depth (Fig. 3A). Average

surface Chl-a was 1.00 ± 0.47 mg m^{-3} and at 5 m this variable was highest (1.72 ± 0.69 mg m^{-3}). Below the subsurface maximum, chlorophyll decreased to 0.47 ± 0.29 mg m^{-3} at 45 m. Like chlorophyll, bacterioplankton increased from the surface (248 ± 73 10^3 cell mL^{-1}) to 5 m depth (557 ± 293 10^3 cell mL^{-1}), then decreased with depth (Fig. 3E). Nitrate concentrations increased strongly with deep from 8.02 ± 2.3 µmol L^{-1} in surface waters to 25.77 ± 3.11 µmol L^{-1} at 45 m. The analyses of water masses show warmer and saltier water compared to the fjord areas (Fig. 2C). An important freshwater-influenced layer (< 5m) is present followed by Equatorial subsurface water (ESSW) in deeper layers.

In northern Patagonia (Puyuhuapi Fjord), freshwater inputs are characterized by the outflow of Cisnes River (Fig. 2B), the maximum month average were registered in spring (272 ± 152 m^3 s^{-1}) and the minimums in February (127 ± 108 m^3 s^{-1} in February). River discharge during sampling period (August) usually has shown intermediate levels of discharge with a monthly average of 193 ± 209 m^3 s^{-1}. The average salinity in surface waters showed high variability along the channel (Fig. 3B). Averages were 29.9 ± 1.14 psu at northern stations but 17.88 ± 1.08 psu in the south; however, in deep layers, salinity profiles were constant (~33 psu). Surface temperatures were similar in the south (9.49 ± 0.30 °C) and north Patagonia (9.08 ± 0.77 °C) and remained stable with depth. Chl-a was highest in surface waters in the south (1.50 ± 0.36 mg m^{-3}) while northern maxima were observed at 10 m depth (0.75 ± 0.23 mg m^{-3}). In both zones, Chl-a and bacterioplankton abundances decreased with depth following the same pattern. Nitrate concentrations in the south of the channel peaked at depths of 50 m (25 µmol L^{-1}) and 150 m (15.28 µmol L^{-1}), but deep-water nitrate concentrations in the north were low compared to values in the south (Fig. 3F). Puyuhuapi Fjord was influenced by estuarine water in surface (<30 m). Below 30 m, modified subantarctic waters (MSAAW) were dominant, with temperatures around 10°C.

The Pia Fjord had the lowest average surface temperature (4.43 ± 0.88 °C), increasing slightly down to 100 m, where it reached an average of 6.92 ± 1.69 °C. Salinity profiles showed lower values and more variable at the surface (28.37 ± 2.62 psu), followed by an increment to 30.39 ± 0.077 psu at 5 m and to 31.54 ± 1.02 psu at 100 m (Fig. 3C). Chl-a ranged from 0.03 to 0.28 mg m^{-3} at the surface and decreased slightly with depth. Bacterioplankton abundances were highest in surface waters (147 ± 54 $x10^3$ cell mL^{-1}) and decreased with depth (48 ± 34 $x10^3$ cell mL^{-1}). Finally, the observed nitrate concentrations were around 11.56 ± 1.57 µmol L^{-1} at the surface and increased slowly to 15.06 ± 0.43 µmol L^{-1} at 100 m depth (Fig. 3G).

Temperature and salinity in the Yendegaia Fjord increased with depth (Fig. 3D). In this fjord, Chl-a decreased following the same trend observed for Pia fjord. Bacterioplankton abundances were highest at the surface (214 ± 70 $x10^3$ cell mL^{-1}) and remained stable below 5 m (175 ± 68 $x10^3$ cell mL^{-1}). The same trend was observed for nitrate (Fig. 3H).

3.2. CDOM and DOC distribution in the water column

In the Biobio River, dissolved organic carbon ranged from 47.70 to 162.10 µmol L^{-1}, with maximum concentrations in surface waters. In Puyuhuapi, DOC varied from 69.73 µmol L^{-1} to 119.12 µmol L^{-1}, with maximum concentrations in intermediate waters. For the Beagle Channel, DOC fluctuated between 60.02 and 104.3 µmol L^{-1}. Overall, the median concentrations were 67.2, 78.8, and 72.5 µmol L^{-1} for Biobio, Puyuhuapi, and Beagle, respectively (Fig 4A). The only significant differences detected by analyzing DOC concentrations were between the Beagle Channel (surface and intermediate layers) and the Biobio River (intermediate depths) (p-value=0.030 and 0.025, respectively).

For CDOM parameters, values of a_{325} were highest in the deep waters of the Puyuhuapi Fjord (3.865 m^{-1}), followed by the intermediate layer of Beagle Channel (1.729 m^{-1}). Significant differences were detected in Biobio River between the intermediate layer and surface (p-value=0.040). Also, differences occurred between Biobio River and Beagle Channel at the surface (p-value=0.005) and in intermediate layers (p-value=0.001) and Puyuhuapi Fjord at the surface (p-value=0.031) and in the deep layer (p-value=0.036). In the Puyuhuapi and Beagle channels, non-significant differences were found for a_{325} among depths.

SCDOM values were highest in the deep waters of the Puyuhuapi Fjord (0.304 nm^{-1}), followed by 0.020 nm^{-1} in Beagle Channel and 0.014 nm-1 in Biobio River (Fig. 4C). On the other hand, values of S_R in Biobio River varied from 1.065 to 2.592, whereas in Puyuhuapi they ranged from 0.480 to 1.477. In the Beagle Channel values of S_R varied from 0.922 to 1.842. In Biobio, the highest SR was estimated for intermediate waters as well as in Puyuhuapi fjord, but for Beagle Channel, the highest S_R values were located in the deepest waters (Fig. 4D). No significant differences were found along the water column within each study area ($p>0.050$). However, we observed significant differences between study areas. Significant changes in S_R at the surface and intermediate layers were found between the Beagle Channel and Puyuhuapi Fjord ($p<0.05$). S_R values of surface waters in Biobio were significantly different from deep and surface Puyuhuapi waters (p=0.018 and 0.029, respectively).

The principal component analysis showed differences between zones (Fig.5). The first principal component represented 43.8% of the variance of environmental parameters

(temperature, Chl-a, microbial abundances; Table 2). This principal axis revealed geographical variability in the case of Puyuhuapi fjord and temporal variability for the Biobio River. In contrast, Pia and Yendegaia fjords were less variable and grouped together. The second principal component (PC2), which explained 25.4% of the remaining variability, represented salinity and nitrate changes (Table 2).

Linear regression between the PC1 (biological variables and temperature) the PC2 scores (representing changes in salinity) and the a_{325} values indicated significant relationships for Biobío River (p-value=0.010 and p-value<0.001, respectively) explaining the 28 and 46% of their respective variability. Linear relationships between PC2 scores and Puyuhuapi Fjord were significant (p-value=0.048, n=12) and explained 34% of the variability. However, no significant relationships were found between the PC2 scores and a_{325} for the Beagle Channel (Table 3). Spearman correlations between DOC and a_{325} by area revealed non-significant correlations, except for the Biobio River (rho=0.637, p-value=0.001, n=21). However, a high positive but non-significant correlation was found at the southern Puyuhuapi stations (rho=0.714, p-value=0.088, n=7). In the case of the Beagle Channel, important correlations were found only for Pia Fjord (rho=0.462, p-value=0.072, n=16; Table 3).

Overall, the stratification parameter varied from 0.02 to 0.78, going from the lowest estimated values (0.02-0.19) at the Beagle channel to intermediate values at Biobio (0.37-0.62) and the highest at Puyuhuapi Fjord (0.78). Particularly heterogeneous conditions were observed in Puyuhuapi with maximum values observed in the southern stations, which contrasted with the northern channel. Surface a_{325} presented a positive and exponential relationship with stratification (0.002+exp (1.453*ns), n=16) explaining the 63% surface

296 CDOM variability (Fig.6A). Average SR (considering all the sampling points per profile)
297 varied along with water column stratification in all study areas. Significant differences were
298 found among zones of study (One-way ANOVA, p=0.007). Average S_R in Puyuhuapi (0.99
299 ± 0.07) was significantly low compared to the Beagle channel (1.43 ± 0.04) and Biobio
300 (1.17 ± 0.20). No differences were found between average SR between Beagle and Biobio.

301

302 **4. Discussion**

303

304 The study of CDOM dynamics is an emergent field of research off the Chilean coast. Other
305 than a recent study on CDOM distribution off central Chile (Vargas et al., 2013) this study
306 is the first report of CDOM variability from the perspective of its optical properties (a_{325},
307 S_{CDOM}, S_R) covering productive conditions in central Chile to subantarctic waters.

308

309 The importance of terrestrial sources of CDOM in our study area is reflected by the
310 significant relationship between CDOM and PC2 scores (which represents river influence)
311 for Biobio River and, less importantly for the Puyuhuapi Fjord (Fig. 5). However, PC2 and
312 CDOM did not correlate in the Beagle Channel.
313 The strong relationship between surface CDOM absorption and DOC in Biobio suggests
314 that chromophoric molecules represent an important fraction of total DOC from terrestrial
315 origins, as previously seen over other continental shelves (Mannino et al., 2008; Shank and
316 Evans, 2011). This was confirmed by the response of the magnitude CDOM to the
317 stratification caused by salinity (Fig.6A). However, there is no conclusive evidence on the
318 importance of river runoff on the CDOM distribution over the entire water column in this

study. Indeed, the highest CDOM concentrations were registered in Puyuhuapi although the river discharge of the Cisnes River was less intense (7-fold in winter season) than the Biobío River (Fig.3). Second, mean CDOM seems to be independent of the water column stability.

Even if no significant differences occurred in surface DOC concentrations among our study areas, the optical parameters of CDOM (a_{325}, S_{CDOM}, S_R) allowed us to identify differences in CDOM between and within zones (Fig. 4). First, Biobio stations presented high levels of DOC, a_{325}, and S_{CDOM} at the surface compared with deeper layers. High S_{CDOM} has been associated with photobleached CDOM (Vodacek et al., 1997; Moran et al., 2000; Stedmon and Markager, 2001). Also, low S_R values were related to the low salinities found in surface waters which were associated with compounds of terrestrial origin (high molecular weight), in accordance with estuarine values reported in previous literature (Das et al., 2017; Helms et al., 2008). Sampling sites in Puyuhuapi Fjord showed the highest a_{325} values in CDOM but the same was not true for DOC concentrations. S_R values were lower in Puyuhuapi for all depths compared to BioBio, suggesting a system strongly influenced by terrestrial organic matter in the water column (even independent of the particular oceanographic conditions during the sampling time) in contrast with the fjords of the Beagle Channel, which were associated to *in situ* produced DOM (SR around 1.5) in subsurface depth layers.

The southern Channel in Puyuhuapi presented the expected CDOM distribution for an estuarine system: CDOM was high at the surface but tended to increase in deep waters in the northern channel. Interestingly, high a_{325} was observed along with a nitrate peak in

343 intermediate layers (Fig. 3B) with higher SR, suggesting potential local production of
344 CDOM decoupled from freshwater input in the southern channel of the Puyuhuapi Fjord.
345
346 The stations in Pia and Yendegaia fjords (Beagle Channel) showed the lowest chlorophyll
347 levels (Fig. 2G,H) and less stratified water column of our study. However DOC
348 concentrations, varied in the same order as Biobio River and Puyuhuapi Fjord (Fig. 4A).
349 The stations in Beagle Channel presented higher DOC and a_{325} concentrations at 10 m
350 compared to surface and deep layers which were unrelated to salinity changes. However,
351 we observed relatively high and stable SR (~1.5) values through the water column
352 compared to the Puyuhuapi Fjord. These findings suggest these fjords to be well-mixed
353 dominated by DOM of low molecular weight and *in situ* biological production (such as
354 zooplankton excretion) as reported by Steinberg et al. (2004) for copepods, euphausiids,
355 amphipods, and salps. However, we do not have enough evidence to draw conclusions
356 about the importance of the zooplankton community and the magnitude of their excreted
357 compounds in these systems.
358 These optical parameters (especially a_{325} and S_R) are simple but useful tools for describing
359 the photochemical/biological processes affecting CDOM. Further experiments using
360 fluorometric methods such as the excitation emission spectra (Hansen et al., 2016) and
361 focusing on key species are needed in order to assess the residence time and fingerprinting
362 of chromophoric components in relation to the dynamics of CDOM, its sources, and its
363 sinks in coastal waters.
364

365 **5. Conclusion**

This study aimed to estimate the impact of terrestrial DOM on the characterization of CDOM in three study areas. S_R concentrations along with a_{325} and S_{CDOM} showed marked differences between the three regions. .Freshwater was mostly responsible for surface CDOM changes and the principal source of chromophoric material input to in Biobio River and Puyuhuapi Fjord, when systems are highly stratified Surface terrigeneous organic matter dominated the dissolved organic pool in Puyuhuapi and was strongly correlated with its colored component. Changes in the average spectral ratio were observed independent of the condition of the water column in Beagle Channel and Puyhuapi suggesting the distribution of CDOM is potentially dominated by biological *in situ* production below the surface freshwater-influenced layer. We conclude that in stratified systems freshwater inputs determine the distribution of surface CDOM, but in well-mixed systems the *in situ* production of CDOM dominates.

Acknowledgements

We thank Claudia Muñoz and Maria Lorena Gonzalez for support in fieldwork. This study was partially funded by LIA MORFUN, Fondecyt grants 1150891 and 1180954, COPAS Sur-Austral CONICYT PIA APOYO CCTE AFB170006, INCAR (FONDAP-CONICYT No15110027), and IDEAL (FONDAP-CONICYT No15150003).

References

Aminot, A., Kérouel, R., 2007. Dosage automatique des nutriments dans les eaux marines. Editions Quae.

Benner, R., Strom, M., 1993. A critical evaluation of the analytical blank associated with DOC measurements by high-temperature catalytic oxidation. Mar. Chem. https://doi.org/10.1016/0304-4203(93)90113-3

Bricaud, A., Morel, A., Prieur, L., 1981. Absorption by dissolved organic matter of the sea (yellow substance) in the UV and visible domains. Limnol. Ocean. 26, 43–53.

Das, S., Das, I., Giri, S., Chanda, A., Maity, S., Lotliker, A.A., Kumar, T.S., Akhand, A., Hazra, S., 2017. Chromophoric dissolved organic matter (CDOM) variability over the continental shelf of the northern Bay of Bengal. Oceanologia 59, 271–282. https://doi.org/10.1016/J.OCEANO.2017.03.002

Del Vecchio, R., Blough, N. V, 2004. Spatial and seasonal distribution of chromophoric dissolved organic matter and dissolved organic carbon in the Middle Atlantic Bight. Mar. Chem. 89, 169–187. https://doi.org/10.1016/j.marchem.2004.02.027

Escribano, R., Schneider, W., 2007. The structure and functioning of the coastal upwelling system off central/southern Chile. Prog. Oceanogr. 75, 343–347. https://doi.org/10.1016/j.pocean.2007.08.020

Fichot, C.G., Benner, R., 2011. A novel method to estimate DOC concentrations from CDOM absorption coefficients in coastal waters. Geophys. Res. Lett. 38, n/a-n/a. https://doi.org/10.1029/2010GL046152

Hansen, A.M., Kraus, T.E.C., Pellerin, B.A., Fleck, J.A., Downing, B.D., Bergamaschi, B.A., 2016. Optical properties of dissolved organic matter (DOM): Effects of biological and photolytic degradation. Limnol. Oceanogr. 61, 1015–1032.

411 https://doi.org/10.1002/lno.10270
412 Haralambidou, K., Sylaios, G., Tsihrintzis, V.A., 2010. Salt-wedge propagation in a
413 Mediterranean micro-tidal river mouth. Estuar. Coast. Shelf Sci. 90, 174–184.
414 https://doi.org/10.1016/j.ecss.2010.08.010
415 Helms, J.R., Stubbins, A., Ritchie, J.D., Minor, E.C., Kieber, D.J., Mopper, K., 2008.
416 Absorption spectral slopes and slope ratios as indicators of molecular weight, source,
417 and photobleaching of chromophoric dissolved organic matter. Limnol. Oceanogr. 53,
418 955–969. https://doi.org/10.4319/lo.2008.53.3.0955
419 Holm-Hansen, O., Lorenzen, C.J., Holmes, R.W., Strickland, J.D.H., 1965. Fluorometric
420 Determination of Chlorophyll. ICES J. Mar. Sci. 30, 3–15.
421 https://doi.org/10.1093/icesjms/30.1.3
422 Hulatt, C.J., Thomas, D.N., Bowers, D.G., Norman, L., Zhang, C., 2009. Exudation and
423 decomposition of chromophoric dissolved organic matter (CDOM) from some
424 temperate macroalgae. Estuar. Coast. Shelf Sci. 84, 147–153.
425 Huovinen, P., Ramírez, J., Gómez, I., 2016. Underwater Optics in Sub-Antarctic and
426 Antarctic Coastal Ecosystems. PLoS One 11, e0154887.
427 https://doi.org/10.1371/journal.pone.0154887
428 Llabrés, M., Agustí, S., Fernández, M., Canepa, A., Maurin, F., Vidal, F., Duarte, C.M.,
429 2013. Impact of elevated UVB radiation on marine biota: a meta-analysis. Glob. Ecol.
430 Biogeogr. 22, 131–144. https://doi.org/10.1111/j.1466-8238.2012.00784.x
431 Mannino, A., Russ, M.E., Hooker, S.B., 2008. Algorithm development and validation for
432 satellite-derived distributions of DOC and CDOM in the U.S. Middle Atlantic Bight.
433 J. Geophys. Res. 113, C07051. https://doi.org/10.1029/2007JC004493
434 Marie, D., Simon, N., Guillou, L., Partensky, F., Vaulot, D., 2000. Flow cytometry analysis

435 of marine picoplankton, in: Diamond, R., DeMaggio, S. (Eds.), Living Color:
436 Protocols in Flow Cytometry and Cell Sorting. Berlin, pp. 421–454.
437 Moran, M.A., Sheldon, W.M., Zepp, R.G., 2000. Carbon loss and optical property changes
438 during long-term photochemical and biological degradation of estuarine dissolved
439 organic matter 45, 1254–1264.
440 Nelson, N.B., Siegel, D.A., Michaels, A.F., 1998. Seasonal dynamics of colored dissolved
441 material in the Sargasso Sea. Deep. Res. Part I Oceanogr. Res. Pap. 45, 931–957.
442 Nelson, N.B., Siegel, D. a, 2013. The global distribution and dynamics of chromophoric
443 dissolved organic matter. Ann. Rev. Mar. Sci. 5, 447–76.
444 https://doi.org/10.1146/annurev-marine-120710-100751
445 Nelson, N.B., Siegel, D. a., Carlson, C. a., Swan, C., Smethie, W.M., Khatiwala, S., 2007.
446 Hydrography of chromophoric dissolved organic matter in the North Atlantic. Deep
447 Sea Res. Part I Oceanogr. Res. Pap. 54, 710–731.
448 https://doi.org/10.1016/j.dsr.2007.02.006
449 Rain-Franco, A., Muñoz, C., Fernandez, C., 2014. Ammonium production off central Chile
450 (36°S) by photodegradation of phytoplankton-derived and marine dissolved organic
451 matter. PLoS One 9, e100224. https://doi.org/10.1371/journal.pone.0100224
452 Saldías, G., Sobarzo, M., Largier, J., Moffat, C., Letelier, R., 2012. Seasonal variability of
453 turbid river plumes off central Chile based on high-resolution MODIS imagery.
454 Remote Sens. Environ. 123, 220–233. https://doi.org/10.1016/j.rse.2012.03.010
455 Schneider, W., Pérez-Santos, I., Ross, L., Bravo, L., Seguel, R., Hernández, F., 2014. On
456 the hydrography of Puyuhuapi Channel, Chilean Patagonia. Prog. Oceanogr. 129, 8–
457 18. https://doi.org/10.1016/j.pocean.2014.03.007
458 Shank, G.C., Evans, A., 2011. Distribution and photoreactivity of chromophoric dissolved

459 organic matter in northern Gulf of Mexico shelf waters. Cont. Shelf Res. 31, 1128–
460 1139. https://doi.org/10.1016/j.csr.2011.04.009
461 Stedmon, C. a., Markager, S., 2001. The optics of chromophoric dissolved organic matter
462 (CDOM) in the Greenland Sea: An algorithm for differentiation between marine and
463 terrestrially derived organic matter. Limnol. Oceanogr. 46, 2087–2093.
464 https://doi.org/10.4319/lo.2001.46.8.2087
465 Steinberg, D.K., Nelson, N.B., Carlson, C.A., Prusak, A.C., 2004. Production of
466 chromophoric dissolved organic matter (CDOM) in the open ocean by zooplankton
467 and the colonial cyanobacterium Trichodesmium spp. Mar. Ecol. Prog. Ser. 267, 45–
468 56.
469 Swan, C.M., Siegel, D. a., Nelson, N.B., Carlson, C. a., Nasir, E., 2009. Biogeochemical
470 and hydrographic controls on chromophoric dissolved organic matter distribution in
471 the Pacific Ocean. Deep Sea Res. Part I Oceanogr. Res. Pap. 56, 2175–2192.
472 https://doi.org/10.1016/j.dsr.2009.09.002
473 Twardowski, M.S., Boss, E., Sullivan, J.M., Donaghay, P.L., 2004. Modeling the spectral
474 shape of absorption by chromophoric dissolved organic matter. Mar. Chem. 89, 69–
475 88. https://doi.org/10.1016/j.marchem.2004.02.008
476 Vargas, C., Arriagada, L., Sobarzo, M., PY, C., Saldías, G., 2013. Bacterial production
477 along a river-to-ocean continuum in central Chile: implications for organic matter
478 cycling. Aquat. Microb. Ecol. 68, 195–213.
479 Vodacek, A., Blough, N. V., Degrandpre, M.D., Peltzer, E.T., Nelson, R.K., 1997. Seasonal
480 variation of CDOM and DOC in the Middle Atlantic Bight: Terrestrial inputs and
481 photooxidation. Limnol. Oceanogr.
482 Yuras, G., Ulloa, O., Hormazábal, S., 2005. On the annual cycle of coastal and open ocean

satellite chlorophyll off Chile (18°–40°S). Geophys. Res. Lett. 32, L23604.
https://doi.org/10.1029/2005GL023946

487 **Table 1. Summary of sampled stations for each study area**

Location	Station	Date	Longitude (ºW)	Latitude (ºS)	Sampling depth (m)
Biobío River	Biobío river	12-11-2013	73.226	36.829	0, 5, 20, 45
Biobío River	Biobío river	12-11-2013	73.226	36.829	0, 5, 20, 45
Biobío River	Biobío river	12-11-2013	73.226	36.829	0, 5, 20, 45
Biobío River	Biobío river	12-11-2013	73.226	36.829	0, 5, 20, 45
Biobío River	Biobío river	13-11-2013	73.226	36.829	0, 5, 20, 45
Biobío River	Biobío river	13-11-2013	73.226	36.829	0, 5, 20, 45
Puyuhuapi fjord	EJb	08-08-2016	72.7052	44.5268	2, 10, 50, 140
Puyuhuapi fjord	EBa	06-08-2016	72.728	44.589	2, 10, 70, 140
Puyuhuapi fjord	EBb	06-08-2016	72.712	44.599	2, 10, 70, 140
Puyuhuapi fjord	ECb	07-08-2016	72.7644	44.7224	2, 10, 50, 100
Puyuhuapi fjord	ESb	09-08-2016	73.084	44.918	2, 10, 50, 100
Puyuhuapi fjord	ESa	09-08-2016	73.106	44.913	2, 10, 100
Beagle Channel	PB	26-07-2017	69.697	54.859	0 , 5, 10, 25, 50, 100
Beagle Channel	P1	24-07-2017	69.661	54.804	0 , 5, 10, 25, 50, 100
Beagle Channel	P2	24-07-2017	69.673	54.769	0 , 5, 10, 25, 50, 100
Beagle Channel	Y1	22-07-2017	68.764	54.860	0 , 5, 10, 25, 50, 100
Beagle Channel	Y2	22-07-2017	68.688	54.898	0 , 5, 10, 25, 50, 100
Beagle Channel	Y3	23-07-2017	68.802	54.849	0 , 5, 10, 25, 50

488

489

490 **Table 2. PCA analysis.** Eigenvectors for the first and second principal components carried

491 out for environmental variables from Biobío River, Puyuhuapi fjord, and Beagle Channel.

Environmental variables	**Principal Component 1**	**Principal Component 2**
Temperature (°C)	0.441	0.133
Salinity (PSU)	-0.157	**-0.707**
Nitrate (µmol L^{-1})	-0.196	**-0.586**
Bacterioplankton (10^3 cell mL^{-1})	**0.450**	-0.220
Synechoccocus sp. (10^3 cell mL^{-1})	**0.508**	-0.295
Chlorophyll (mg L^{-1})	**0.531**	-0.067
Cumulative variance explained (%)	43.80	69.20

492

493

Table 3. Summary regression parameters and Spearman correlation. Significant values are presented in bold. For the regression procedures, a natural log transformation was applied to a_{325} values.

	PC1				PC2					DOC		
CDOM	Intercept	Slope	R^2	p-value	Intercept	Slope	R^2	p-value	n	Rho	p-value	n
Overall Biobio	0.897	0.136	**0.277**	**0.010**	0.001	0.168	**0.46**	**0.000**	21	0.592	**0.002**	**24**
Overall Puyuhuapi	1.864	0.069	0.009	0.771	0.590	0.304	**0.34**	**0.048**	12	0.196	0.482	15
Stations Boya	1.990	-0.436	0.368	0.202	0.653	0.446	0.58	0.077	6	-0.262	0.536	8
Stations South	1.614	0.412	0.295	0.266	0.543	0.256	0.26	0.300	6	0.714	0.088	7
Overall Beagle	1.363	0.172	0.007	0.696	0.086	0.070	0.01	0.653	26	0.271	0.154	29
Pia Fjord	0.769	-0.317	0.035	0.538	0.247	-0.163	0.10	0.288	13	0.462	0.072	16
Yendegaia Fjord	2.860	1.410	0.291	0.087	-0.052	0.577	0.08	0.402	13	0.099	0.751	13

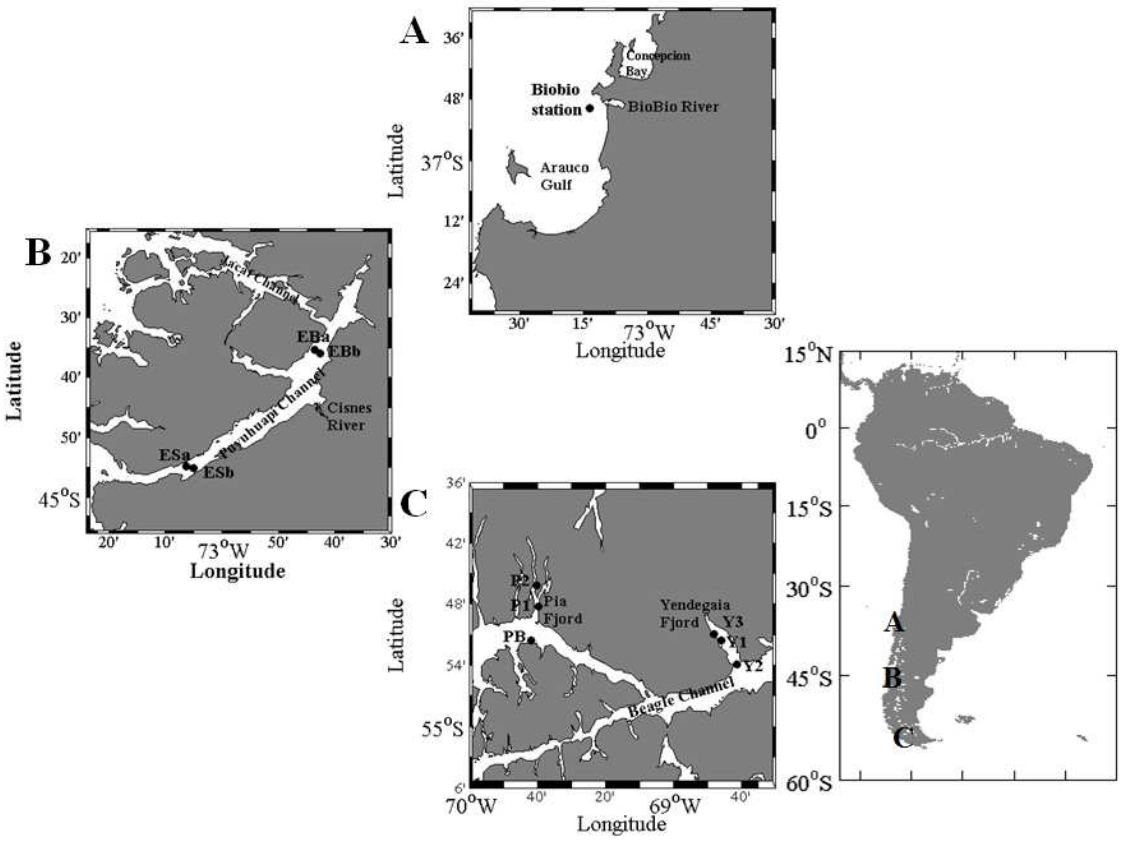

499

500 **Figure 1.** Location of oceanographic stations in the three study areas. A) Biobio River, B)

501 Puyuhuapi fjord, and C) Beagle Channel.

502

503

504

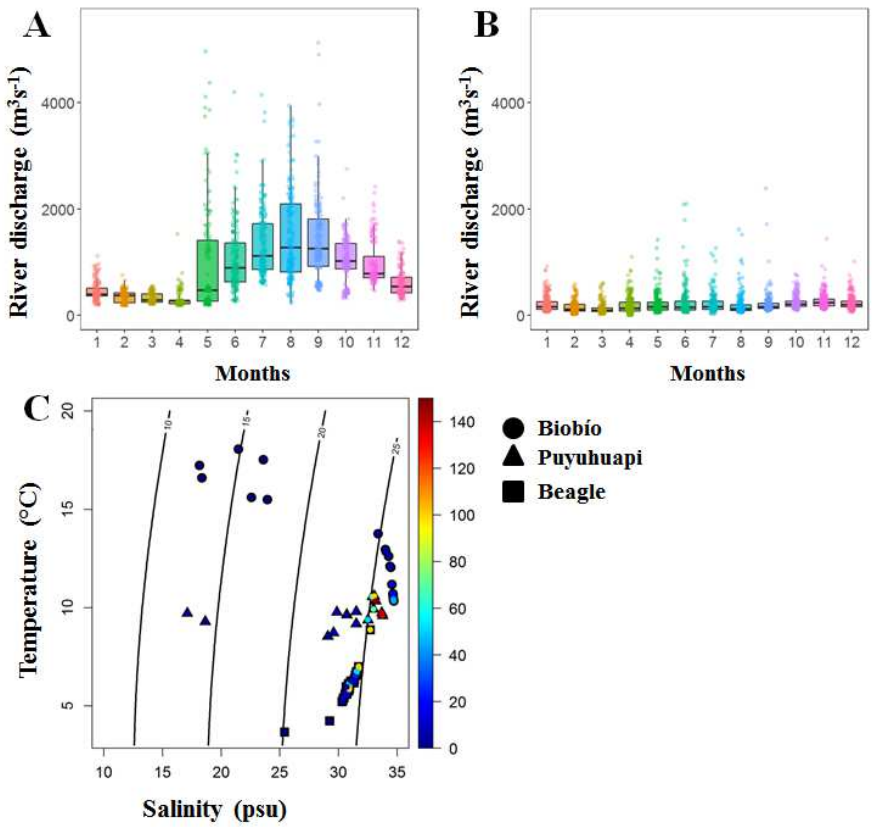

505

506 **Figure 2. River discharge and T-S diagram for the study sites.** A) Annual variability of
507 Biobio River discharge (Central Chile) and B) Cisnes River (Puyuhuapi Fjord, northern
508 Patagonia). No data was available for the Beagle Channel. C) T-S diagram from the
509 sampling depths per study area. Error bars indicate standard deviations.

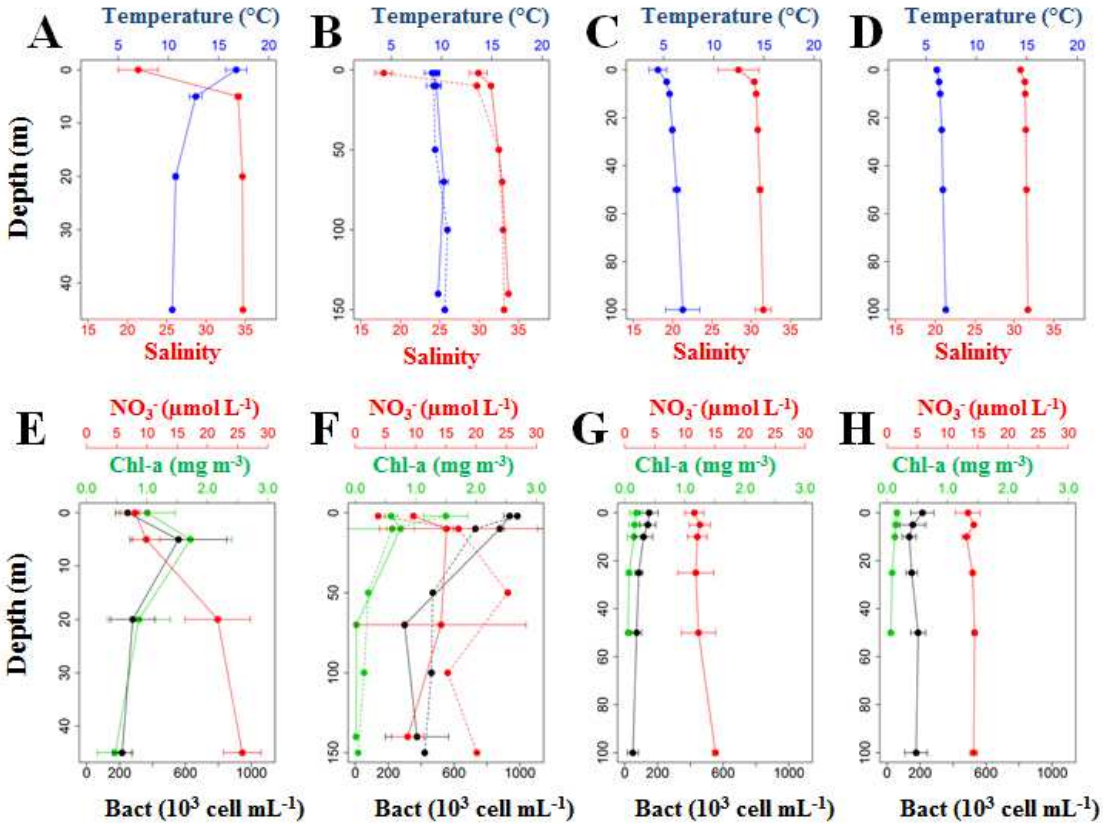

Figure 3. Oceanographic conditions in the three study areas during sampling. Average profiles of temperature, salinity, Nitrate, Chl-a and Bacterioplankton abundance for A,E) Biobío River, B,F) Puyuhuapi Fjord (dashed lines represent northern channel stations), C,G) Pia Fjord (Beagle Channel) and D,H) Yendegaia Fjord (Beagle Channel).

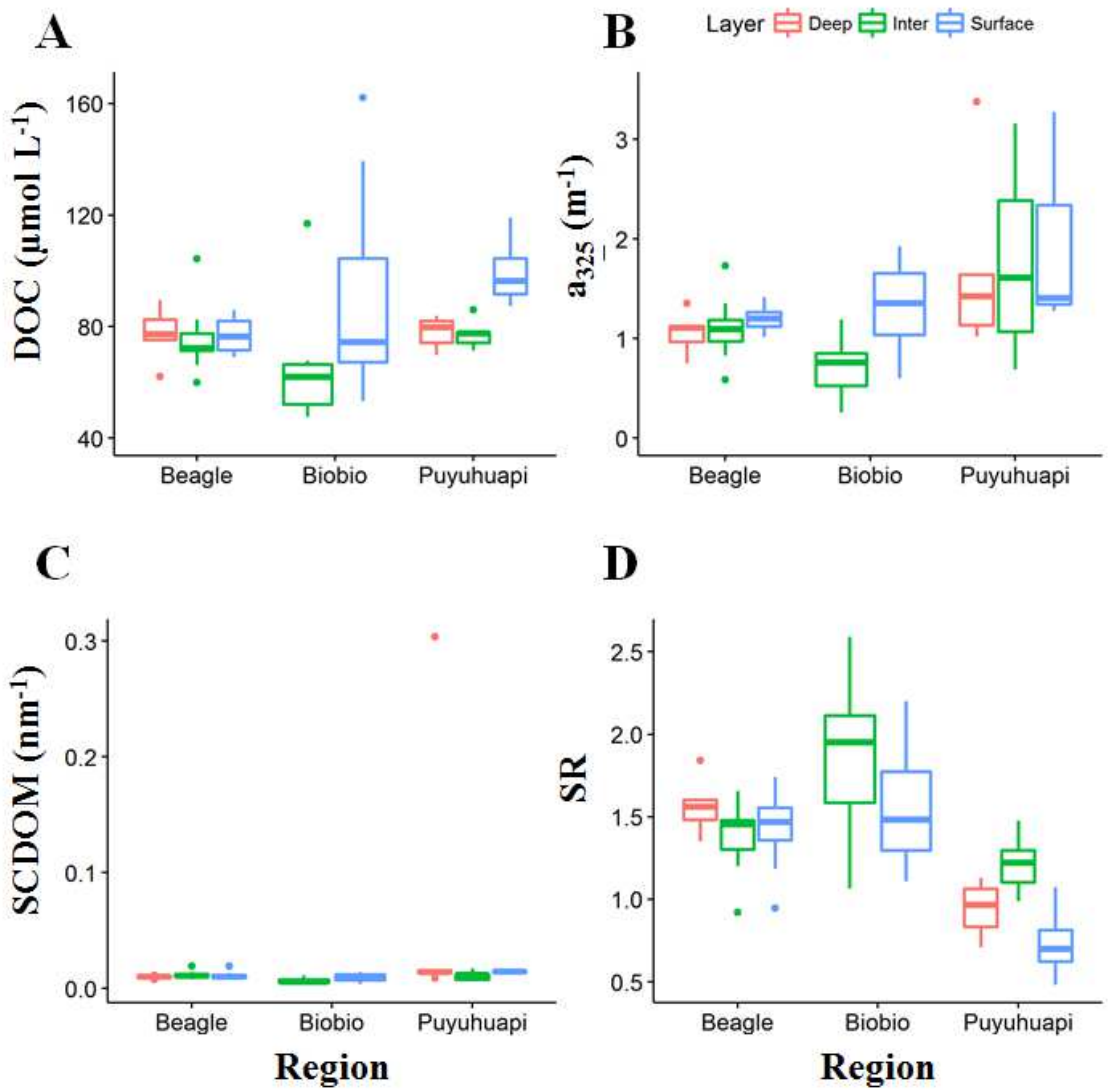

518

519 **Figure 4. Boxplot of dissolved organic matter and their optical parameters per study**

520 **area.** Deep (red), intermediate (green), and surface (blue) depth layers. Boxes represent the

521 interquartile range. Horizontal lines indicate the median of the values.

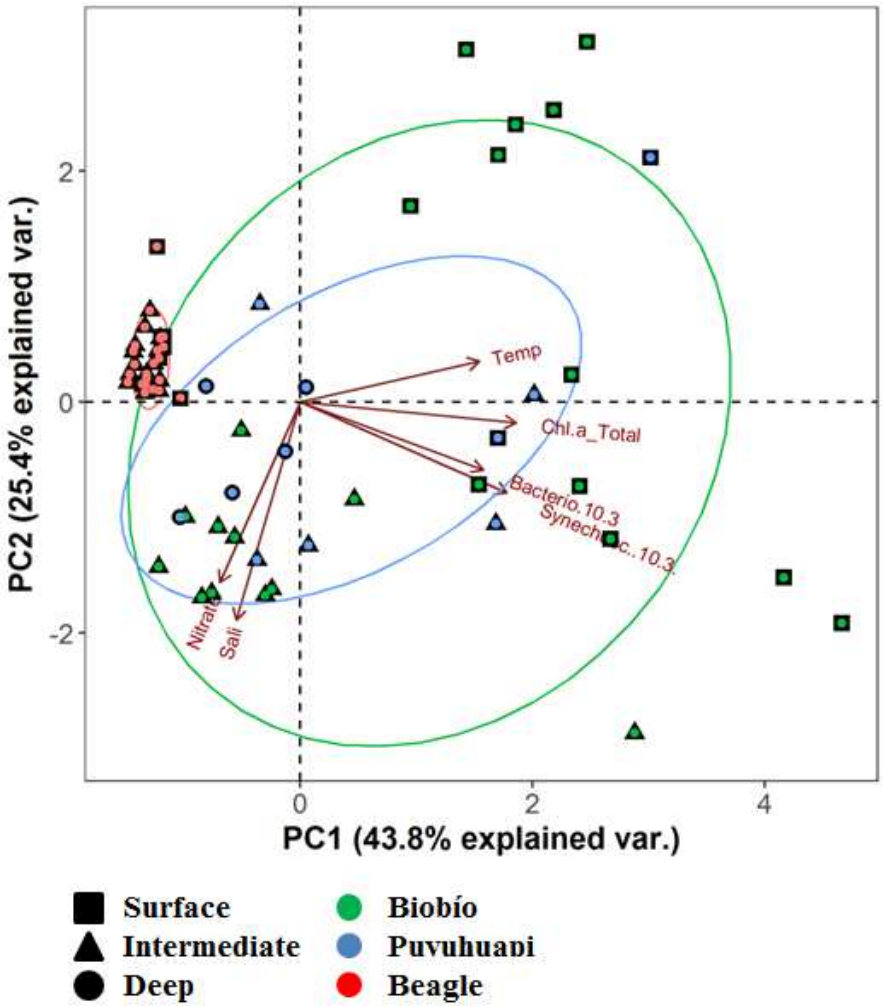

522

523 **Figure 5.** Biplot of principal components analyses (PCA) for environmental variables,
524 DOC, and optical parameters in the three study areas. Biobío River (green dots), Puyuhuapi
525 fjord (blue dots), and Beagle Channel (red dots). Squares represent surface values (0-10 m);
526 triangles show intermediate depths (>10-70 m), and circles mark deep values (>70 m).

527

528

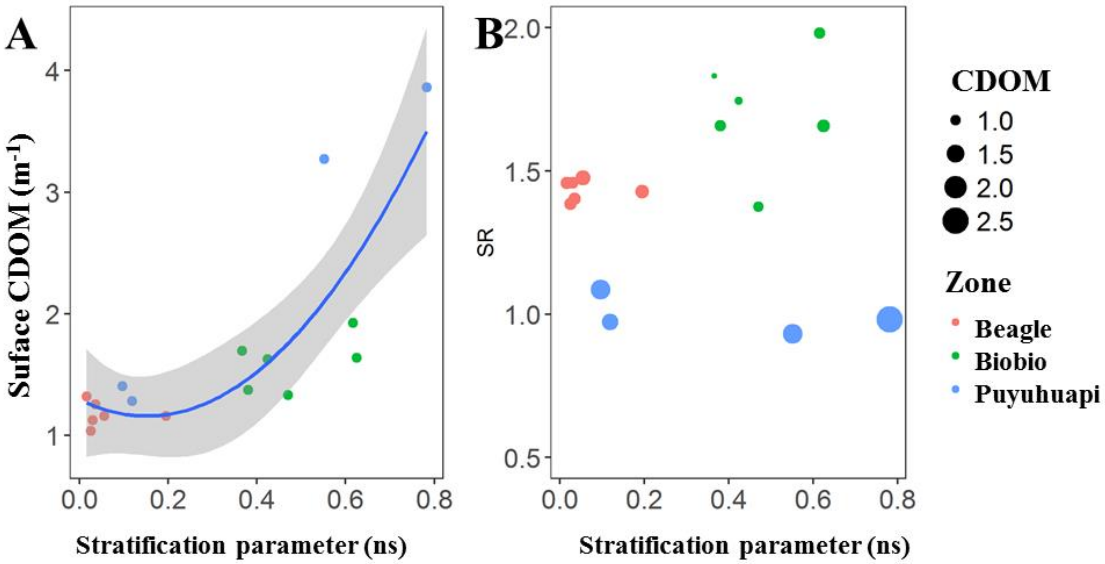

Figure 6. Relationship between stratification and CDOM properties. A) Exponential relations of stratification parameter against surface CDOM absorbance (Surface CDOM= 0.002+exp(1.453*ns), R^2= 0.63). B) Stratification parameter and average spectral ratio per profile (SR), Size of the points represent the mean concentration of surface CDOM.